SMART: Space and Airborne Mined Area Reduction Tools - Presentation

Yann Yvinec[a], Dirk Borghys[a], Marc Acheroy[a],
Helmut Süß[b], Martin Keller[b], Milan Bajic[c], Eléonore Wolff[d],
Sabine Vanhuysse[d], Isabelle Bloch[e], Yong Yu[e] and Olivier Damanet[f]

[a]Signal and Image Centre - Royal Military Academy, Av. de la Renaissance 30, Brussels, Belgium, yvinec@elec.rma.ac.be, Dirk.Borghys@elec.rma.ac.be, Marc.Acheroy@elec.rma.ac.be
[b]Institute of Radio-Frequency Technology and Radarsystems - DLR - German Aerospace Centre, Oberpfaffenhofen, Germany, Helmut.Suess@dlr.de, martin.keller@dlr.de
[c]Scientific Council, Croatian Mine Action Centre, Sisak, Croatia, milan.bajic@zg.tel.hr
[d]IGEAT, Université Libre de Bruxelles (ULB)
Avenue Franklin Roosevelt, 50, Brussels, Belgium, ewolff@ulb.ac.be, svhuysse@ulb.ac.be
[e]TSI, Ecole Nationale Supérieure des Télécommunications - CNRS URA 820,
Rue Barrault 46, Paris, France, isabelle.bloch@enst.fr, yuyong@tsi.enst.fr
[f]TRASYS SPACE, Avenue Ariane, 7, Brussels, Belgium, olivier.damanet@trasys.be

Abstract

This paper presents SMART, a European project that intends to help Mine Action Centres (MAC) in their task of area reduction by providing a GIS-based environment with specific tools to ease the interpretation work of the operator. Using multi-spectral optical data and SAR data obtained during a flight campaign in Croatia and satellite data from before the conflict, the tools will help the land-cover classification and the detection of indicators of mine-suspected areas. The results of these tools will be given to a data fusion module that will summarise all data and contextual information available to facilitate the creation of a 'map of danger'.

SMART started in 2001 for a duration of 3 years.

1 Introduction

The use of airborne and/or space-borne tools with optical and microwave sensors seems to be a promising approach to improve the general mine action assessment and area reduction. The usefulness of such tools has already been studied; the possibility to analysis automatically a large amount of data and ease a visual analysis is among their advantages [5] [6].

It is therefore the goal of the project to develop adapted data understanding and data processing tools for improving efficiency and reliability of general mine action assessment. The goal of SMART is not to detect landmines or minefields but help reducing mine-suspected areas. SMART is due to end in 2004.

2 Functional description

SMART functional description is given in figure 1.

The use of the SMART environment is planned as follows. The end-user, a MAC, defines the tasks, the target regions and the required and expected results and provides mine action databases, maps and auxiliary contextual data (described in section 3). A data provider collects the sensor data (described in section 4) and makes them available.

Before launching the SMART environment, the operator can run commercial software on the data. Such software can be used to perform a classification or a change detection between data from before and after the time period when the minefields were laid. The results of this can be read within the SMART environment.

Within the environment the operator can run the SMART detectors of indicators of mine-suspected areas and edit their results. The list of indicators, with an associated list of detectors, is given in section 5.

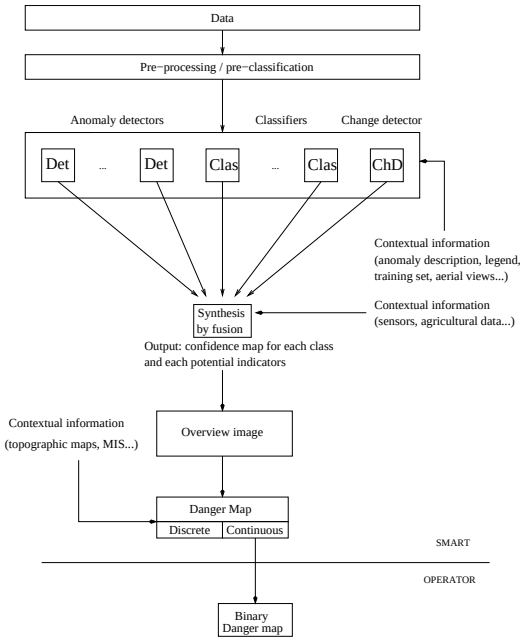

Figure 1: SMART functional description

The operator can use any external information available, such as prints of aerial views, on some specific areas with around 10 to 15 cm resolution, collected during the same flight campaign as for the optical and SAR data.

The operator can use GIS tools to perform some specific analysis: visual identification of some features, identification of some indicators.

The operator can run the module *Synthesis by fusion*, briefly described in section 6, to get maps of confidence for each class and merge these maps into one overview image.

From this the operator can produce discrete and continuous 'danger maps'that are described in section 7. These maps can help the analysis. For instance after studying the maps, the operator can decide to focus on some area. The operator can threshold the continuous 'map of danger' to get a binary map.

The operator provides a report (that may contain the discrete 'danger map', the continuous 'danger map' and the binary map) to the user who will make the area reduction decision.

The following sections describe in more details the different parts of this environment.

3 Expert and contextual knowledge

The expert knowledge is the information obtained from the end-user, i.e. CROMAC (Croatian Mine Action Centre), that will help the development of the SMART tools. It includes:

- Knowledge of the overall mine situation in Croatia, allowing the selection of relevant test and validation areas. Three test areas were selected in mine-suspected zones so as to represent the landscape diversity of the country. A supplementary area, with characteristics similar to one of the test areas, was chosen to implement the global validation of the project.

- Knowledge about the way area reduction is currently performed in the country to ensure that the SMART environment and tools correctly fit with current procedures.

- An analytic assessment of the mine contamination in the test areas, and knowledge about the mine laying strategy. Based on the analysis of military documents, it resulted in the production of reports and maps showing the probable location of minefields, lines of mines, and groups of mines.

- A general description and an expert assessment of the vegetation in the form of a visual interpretation of the images supported by field approval. The in-depth analysis of the vegetation features permits to understand the changes that occur when the land is abandoned, and to focus on the relevant ones, in agricultural zones or in semi-natural vegetation.

- Agricultural data to help interpret the remotely sensed images.

- Information on soil properties in the test areas. Differences in soil colour, moisture and texture can help to explain differences in spectral signatures.

- Information on mine situation and activities related to demining. CROMAC is keeping and updating a Mine Action and Geographic Information System (MAGIS) that contains useful elements for the SMART environment, in particular: mine-suspected areas, mine records for which the co-ordinates are available, cleared areas, cleared areas checked by quality insurance, mine accidents and incidents.

Contextual information has been gathered during two field missions in Croatia. It includes:

- The general description of the geographic features, land cover and land use of the test areas. These elements provide a better understanding of the landscape and ease the interpretation of the images.

- The description and location of potential indicators, which were visually inspected, photographed and represented in the form of a GIS vector layer.

- The building of a training and validation set for

supervised classification. For each sample area, a number of observations pertaining to features of the vegetation were noted down, e.g. the vegetation type, cover rate, and height.

4 The data

Three different airborne sensors were used to collect remote sensing data of all four test areas: DLR's experimental synthetic aperture radar (E-SAR) collected SAR data in X-, C-, L-, and P-band (fully polarimetric and interferometric in L- and P-band). Optical scanner data were recorded by the Daedalus multi-spectral scanner in 11 different channels, ranging from visible blue to thermal infrared. Additionally, very high resolution colour infrared aerial views were collected by a RMK camera (Zeiss ReihenMessKammer), covering the spectral range between near infrared and green. The Daedalus and the RMK data were collected from 300m above ground. The E-SAR's recording altitude was 3000m above ground.

Due to the very low sensor altitude, the original RMK aerial views have a spatial resolution of just 3-5 centimetres. A3 paper prints which have a spatial resolution of 10-15cm are mainly used to help the user by the interpretation of the E-SAR and Daedalus data and processing results. Georeferenced Daedalus data with 1m resolution are available, the final data set was mosaicked from several georeferenced data stripes. E-SAR data are available in georeferenced form (multilook amplitude data) and as SLC (single look complex) data in slant range geometry. The spatial resolution depends on the radar band: georeferenced X-band (9.6GHz) and C-band (5.3GHz) data have 1.5m resolution, L-band (1.3GHz) data has 2.0m and P-band (450MHz) data has 4.0m resolution. For SLC data the spatial resolution is the same in slant range direction, but it is higher by a factor of 2.5 in azimuth direction (flight direction). A polarimetric and interferometric analysis of E-SAR data is only possible with SLC data, the results can be georeferenced afterwards.

A combination of optical and SAR sensors was considered because these sensors deliver complementary information about the ground. While optical data show information about the reflectance of the uppermost part of the vegetation (or other objects), SAR data is able to penetrate through vegetation to a certain amount, depending on the wavelength. While X-band only penetrates through some centimetres of vegetation, P-band is able to penetrate through a forest.

KVR images (visible band, panchromatic, spatial resolution of 2m) of before the war were obtained for the test-sites. They are used for change detection.

5 Potential indicators of minefields

With the expertise of CROMAC and two field missions in the test areas, a list of potential indicators of mine-suspected zones has been established.

This list is evolving regularly and currently includes (but is not limited to):

- Trenches and man-made embankments (remains of military positions that had to be protected)
- River banks (natural obstacles to be reinforced by mines)
- Bridges, including destroyed ones (important strategic points)
- Tracks that are no longer in use (potentially because of fear of mines)
- Agricultural areas that are no longer in use (ditto)
- Shores of ponds (mined to limit access)
- Edges of forests (forests used as shelters by military)
- Power lines (strategic features)
- Soft edges of hardtop roads (used for the progress of military vehicles)

Specific detectors are being built to extract these features. Some of them are described in the next subsections.

In addition to the indicators in the above list, indicators requiring external knowledge were also identified, for instance:

- Mine accidents/incidents (from Mine Action Geographic Information System)
- Mine records (ditto)

5.1 Supervised per-region classification

A supervised per-region classification was performed on 10 of the 11 available optical channels (only the 425-450nm channel was discarded), and neo-channels created on the basis of the raw data, namely principal components, NDVI, and texture images. It allowed the detection of a number of indicators:

5.1.1 River banks, shores of ponds

The class *water* is highly separable from the other classes and has a kappa of 0.97. Since the river can rather easily be classified, it is possible to extract its banks in a further step. Ponds are differentiated from rivers thanks to a shape criterion.

5.1.2 Agricultural areas no longer in use

The difference in vegetation type and texture between cultivated and uncultivated plots can be highlighted thanks to classification, and preliminary results are promising (fig 2). In order to differentiate former agricultural land that is currently neglected from land that was not cultivated even before the conflict, change detection will be performed using Daedalus and KVR data.

5.1.3 Edges of forests

Per-region classification gives fairly good results for the class *forests*, with a kappa of 0.81. However, confusion exists between forests and adjacent former agricultural land covered with bushy vegetation after several years of neglect. This confusion can be overcome by performing the same type of classification on KVR images recorded just before or at the beginning of the conflict, when the forests have cleaner contours.

Alternatively, we have introduced a new clustering algorithm derived from the techniques of probabilistic modeling which maximizes an award function on the data partition. We have also shown that the proposed framework can integrate easily the spatial information. However, it should be remarked that the good performance of forest boundary and bush bands comes from the high quality of their spectral signatures on Daedalus data.

5.1.4 Soft edges of hardtop roads

Hardtop roads can be highlighted thanks to classification, but there is a risk of confusion with other gray surfaces like graveled yards or slate roofs. Here again, the confusion can be overcome by using non-spectral information, i.e. a shape criterion. The kappa for this class is 0.87. A buffer can be used to extract the soft edged of the hardtop roads.

5.2 Detector of aligned poles

Since the area beneath power line is often mined for strategic reasons, a specific tool has been designed to detect power line poles. The possibility to extract the power line positions from maps is seen as not being optimal due to two reasons. In Croatia many of the topographic maps were created in the 70s and don't show the actual situation. Also, when dealing with large areas, the manual extraction of power lines from maps becomes very time consuming, while an automatic processing tool does not need much interaction.

In the multi-spectral Daedalus scanner data, power lines and power line poles cannot be detected reliably due to the small diameter of cables and poles. In E-SAR data the cables show a strongly direction dependent behaviour. They are clearly visible if the power line runs in flight direction but cannot be seen for other directions. Due to their rotation symmetry, the power line poles are well suited for an automatic extraction from the data.

Vertical poles show strong backscatter in co-polar channels due to double reflection on the ground and the pole, especially at longer wavelengths like at P-band. To discriminate poles from tree trunks, a second parameter is used. L-band cross-polar data strongly interact with volume scatterers like the crowns of trees and show a strong backscatter there. Poles are no volume scatterers and so their cross-polar return in L-band is very low.

A mask of all objects is created which show high backscatter in co-polar P-band and low backscatter in cross-polar L-band. Then an algorithm based on the Hough transform is applied to detect aligned patterns within these candidates, using the knowledge of the average distance between two poles (fig 3).

5.3 E-SAR polarimetric decomposition and classification

The entropy/alpha decomposition method [4] was used to extract polarimetric information of L- and P-band SLC SAR data. Three different scattering mechanisms can be extracted which are described by the three eigenvalues and eigenvectors of the 3x3 coherency matrix. The eigenvalues show the intensity and the eigenvectors show the physical nature of the backscatter.

Several parameters can be extracted from the eigenvectors and eigenvalues, the most important are the entropy H which reflects the dominance of one scattering mechanism over the others and therefore the degree of randomness, and the a-angle which is a measure for the scattering mechanism itself. The range of the entropy lies between 0 (low entropy, only one scattering mechanism) and 1 (high entropy, three scattering mechanisms of similar strength). The a-angle can have values between 0 and 90. a=0 means that there exists an odd number of reflections (e.g. single bounce scattering from the ground). An increase of the a-angle is a sign for a change of the scattering properties to dipole scattering (a=45) and finally to an even number of reflections (double bounce, a=90).

The information content of the results of a H/A/a decomposition is very different from regular intensity data of SAR or optical sensors. It needs more interpretation than intensity data but on the other hand contains very useful information, which is independent of the intensities. Such independent information can

help in separating classes which appear very similar in optical and SAR amplitude data.

5.4 Detector of abandoned roads

The idea is to detect roads on the KVR image and the Daedalus image and to compare them. For the single-channel KVR image a classic line detector [8] was used. For the Daedalus image we used a line detector based on multi-variate statistics [3] and applied it on the channels where roads appear as bright lines. Figure 4 shows the results superposed on one Daedalus channel. A few false alarms still persist and these should be eliminated. The method allows to find an abandoned road as well as en newly constructed road.

5.5 Detector of ploughed fields

In ploughed fields, on the Daedalus image a parallel linear structure is found while, in unused fields, structure is more random due to random distribution of vegetation. The idea is to detect regular-shaped surfaces that might correspond to fields and to class them according to whether they contain parallel structures. A multi-variate edge detector [2], initially developed for polarimetric SAR images, was used. It is based on a Hotellings T^2 test for difference of means. For selecting possible fields, the edge detector's response with a high threshold is used and a watershed algorithm is applied to find closed regions. Only regions that are sufficiently compact are kept. Within each selected region the threshold for the edge detector is searched that mimimizes the variance of edge directions within the region. This threshold is used to create a binary edge image on which a Hough transform is applied. The ratio R_H between the maximum of the Hough transform and the second maximum (found for a different direction than the first one) is used as a measurement of presence of a parallel structure. Two thresholds $T_1 < T_2$ were defined and used as follows for classifying the selected regions: if $R_H \geq T_2$ the regions contains parallel structure and is probably a used field. For $R_H \leq T_1$ the region has many edge directions and can be abandoned. If $T_1 < R_H < T_2$ there is doubt and supplementary evidence is needed to reach a decision. Results are shown in fig. 5. Some fields were not selected. Most used fields that were selected are either classified as containing parallel structure or as 'doubt'. The unused fields are either classified as 'no-parallel-structure' or as 'doubt'.

5.6 Road tracking experiment

Curvilinear structure is an anomaly feature, e.g., shores of rivers, tracks that are no longer in use, irrigation channels, etc.

One of our contributions is that we have designed a filter detecting road direction while reducing the noise which seems to be insensitive to the clutters caused by local factors, e.g., grass which covers the tracks.

To detect the road direction on an image, the Hessian matrix is calculated after smoothing convolution.

With the assumption that the change perpendicular to the boundary is much bigger than those along other directions, we can use the unit eigenvector corresponding to the eigenspace of bigger eigenvalue for Hessian matrix to approximate the normal direction of the road. There are several reasons for us to do so. The most important one is that such feature representation is invariant to linear transformation of measurements. Therefore, it is possible to detect uniformly the curvilinear structures with different magnitudes of gradient filtering. It also avoids to introduce some iterative procedure (e.g., rotative projection computation) whose performance and computation complexity depend on the sampling step size.

Then the principal component analysis is applied to optimize the road direction within a local window. This is very important for the initialization of tracking seed.

To complete the tracking, we have adopted the same Kalman filter as in [13] except that the observation vectors consist of the two side boundaries of the road and their norm directions instead of the profile feature.

Experiments have been carried out to verify the correctness of our idea. Fig. 6 shows two examples: one is on a main road and the other on a small path. Both of them are successful. The detection result on the small path is more interesting since it belongs to one of the potential anomaly indicators and our method is insensitive to the clutter generated by wild grasses. However, we have also noted during the experiments that on another branch of the main road in the same scene where shadow effect is dominant, the tracking path deviates from the true one. For the moment, we think it may be caused by the unimodal assumption of the Kalman filter. Then some other methods such as 'particle filtering' techniques [7] have to be explored.

6 Synthesis by fusion

The aim of this module will be to combine the results of classifications and detectors in order to provide

a global classification with confidence degrees for each class at each point or region to be given as input for the construction of danger maps. The main approach that is being investigated is belief function theory [11, 12], since it allows us to model in a natural way the ambiguities and imperfections inherent to each classifier or detector. We are developing two approaches, an unsupervised one and a supervised one.

In the unsupervised approach, each result of the previous step is interpreted as a set of hypotheses, which can be disjunctions of classes of interest. This occurs in particular if a classifier is not able to distinguish between two classes. Then the frame of discernment (i.e. the set of structures of interest) is derived automatically as the set of intersections between the hypotheses output by several classifiers and detectors, similarly as in [9]. These intersections constitute actually the singletons, and each original hypothesis can then be reinterpreted as a disjunction of these singletons. To avoid too many classes, very small classes are eliminated, since they are usually not significant. Mass functions are then defined on each hypothesis according to the numerical answer provided by the classifiers and detectors. The combination is performed using Dempster's rule in unnormalized form and decision is taken according to the maximum belief rule.

In the supervised approach, we rely on some ground truth information, derived from on-site observations and from RMK images, to define the structures of interest and the frame of discernment. Then in each classification, we compute the confusion matrix according to the ground truth information. Classes that are often confused are then grouped together and considered as one compound hypothesis. This explicit modeling of the ambiguities results in less conflict during the combination [1, 10]. Additionally, we derive discounting factors from the individual classification results that represent the reliability of each classifier for each class. Masses are estimated as in the unsupervised approach, and are then discounted using these factors [12] before combination.

In both approaches a final regularization step is to be introduced in order to achieve a better spatial consistency. This is performed at the decision level, by checking that a decision at one pixel is consistent with the one at neighbour pixels.

7 'Danger maps'

'Danger maps' are a way to put together all the information available and obtained through the SMART tools in order to give the operator a global vision of the situation. Two 'danger maps' will be produced for each test area, i.e. a discrete map and a continuous map.

The discrete map is a boolean danger/no danger map that shows all the indicators that have been detected, with buffers materialising their respective danger zones. These buffers are drawn according to the military logic behind the mine-laying strategy around the indicators (e.g. up to 200 meters from a trench, in the direction of the other warring party). Unused fields are also marked since they are likely to be mined. Safe zones such as residential areas or cultivated fields appear as 'no danger' zones (fig 7).

To produce the continuous map, a distance image is generated for each indicator. A function is then designed to rescale the values of each distance image, taking into account the variations in the degree of danger as distance to the indicator increases. The resulting images are considered as factors. They are standardised to a continuous scale, hence allowing us to compare and combine them. Thanks to a pairwise comparison technique, a set of factor weights that sum up to 1.0 is generated, and a factor weight representing the relative danger of the indicator is assigned to each factor. The safe zones are considered as constraints and retain their 'hard' Boolean character, with a weight value of 0 inside and 1 outside. A weighted average of the factors is then performed.

The hard Boolean decision of defining a location as absolutely dangerous or not is avoided, and each location is given a value representing its 'degree of danger'.

8 System architecture

The GIS-based environment of the SMART system will be built on the ESRI ArcGIS Desktop software. The developed management and user-interface module connect the user at the one end and the data at the other end. Besides the collected space and airborne data (section 4), and the data from the Mine Information System (section 3), a specific database was designed to store and manage the information from expert and contextual knowledge: vegetation, agriculture, land cover and land use, ground observations, list of potential locations and anomalies, land-cover classes, how suspected minefield presence can be inferred from that information.

The dedicated user-interface module will provide a user-friendly environment to query, analyse and map all data; and to easily run the SMART and GIS tools to derive all needed information to achieve the 'danger

maps' (section 7).

9 Conclusion

This paper presents the project SMART and its current status. Future work includes the continuation of the design and implementation of the detectors of indicators and the classification tools. The module *synthesis by fusion* is still under development and the concept of 'danger maps' have to be tried on a larger amount of data.

Each tool is to be validated in a progressive way in order to include the end-user's comments into the development stage. In addition a blind validation involving mine clearing will be used to assess the merits of the method and the improvements due to the tools.

Acknowledgments

This work is performed in the scope of the European project **SMART: Space and Airborne Mined Area Reduction Tools** (IST-2000-25044). It is cofunded by the European Commission. The project is coordinated by TRASYS (BE) and Renaissance/RMA (BE). The project partners are CROMAC (HR), DLR (DE), ENST (FR), ixl (DE), Renaissance/RMA (BE), RST (DE), TRASYS (BE), ULB (BE) and Zeppelin (DE). For more information see:
http://www.smart.rma.ac.be/

References

[1] I. Bloch, "Some Aspects of Dempster-Shafer Evidence Theory for Classification of Multi-Modality Medical Images Taking Partial Volume Effect into Account," *Pattern Recognition Letters*, No 8, Vol. 17, pp. 905-919, 1996.

[2] D. Borghys and V. Lacroix and C. M. Acheroy, "A Multi-Variate Contour Detector for High-Resolution Polarimetric SAR Images," *Proc. ICPR 2000, Barcelona*, Vol. 3, pp. 650-655, Sep 2000.

[3] D. Borghys and V. Lacroix and C. Perneel, "Edge and Line Detection in Polarimetric SAR Images," *Proc. ICPR 2002, Quebec*, Vol. 2, pp. 921-924, Aug 2002.

[4] S. Cloude and E. Pottier, "An Entropy Based Classification Scheme for Land Applications of Polarimetric SAR," *IEEE-GRS*, Vol.35, No.1, January 1997.

[5] P. Druyts, Y. Yvinec, M. Acheroy, "Usefulness of semi-automatic tools for airborne minefield detection, " *Clawar 98 -First International Symposium*, pp. 241-248, Brussels, 1998.

[6] P. Druyts, Y. Yvinec, M. Acheroy, "Image processing tools for semi-automatic minefield detection," *ORS99, Second International Symposium on Operationalization of Remote Sensing*, Enschede, Netherlands, August 1999.

[7] M. Isard and A. Blake, "CONDENSATION-conditional density propagation for visual tracking," *Int. J. computer Vision*, No 1, Vol. 29, pp. 5-28, 1998.

[8] V. Lacroix and M. Acheroy, "Feature extraction using the constrained gradient," *ISPRS Journal of Photogrammetry & Remote Sensing*, No 2, Vol. 53, pp. 85-94, 1998.

[9] S. Mascle and I. Bloch and D. Vidal-Madjar, "Application of Dempster-Shafer Evidence Theory to Unsupervised Classification in Multisource Remote Sensing," *IEEE Transactions on Geoscience and Remote Sensing*, No 4, Vol. 35 , pp. 1018-1031, 1997.

[10] N. Milisavljevic and I. Bloch, "Fusion of Anti-Personnel Mine Detection Sensors in Terms of Belief Functions, a Two-Level Approach", *IEEE-SMC*, 2003.

[11] G. Shafer, "A Mathematical Theory of Evidence", *Princeton University Press*, 1976.

[12] P. Smets, "The Combination of Evidence in the Transferable Belief Model," *IEEE-PAMI*, No 5, Vol. 12, pp. 447-458, 1990.

[13] G. Vosselman and J. de Knecht, "Road tracing by profile matching and Kalman filtering," *Proceedings Workshop on Automatic Extraction of Man-Made Objects from Aerial and Space Images*, pp. 265-274, Gruen, A., and O. Kuebler, and P. Agouris, editors, Birkhaeuser, Basel - Boston - Berlin, publisher, 1995.

[14] Y. Yu and I. Bloch and A. Trouvé, "A Unified Unsupervised Clustering Algorithm and its First Application to Landcover Classification," *ICASSP 2003*, Hong-Kong, China, 2003.

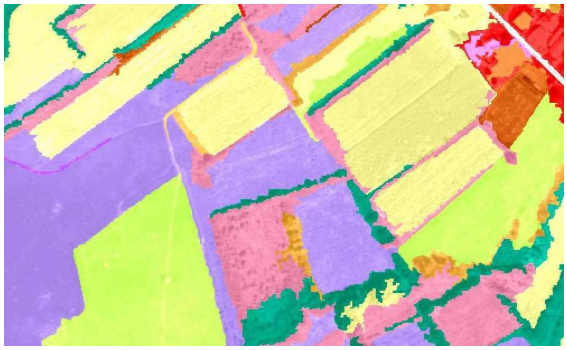

Figure 2: Per-region classification: cultivated areas appear in yellow and green, while uncultivated areas appear in violet and light red.

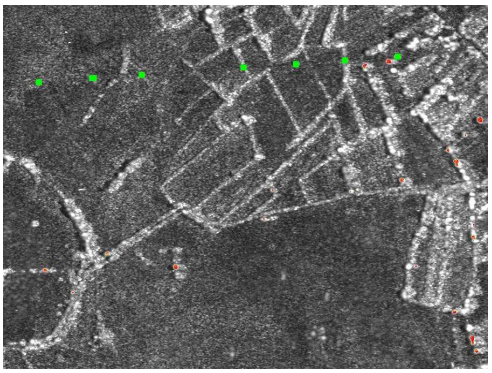

Figure 3: Result after Hough-transform. The mask of the extracted power line poles was searched for an appearance along a row. Red shows candidates and green the detections along a line.

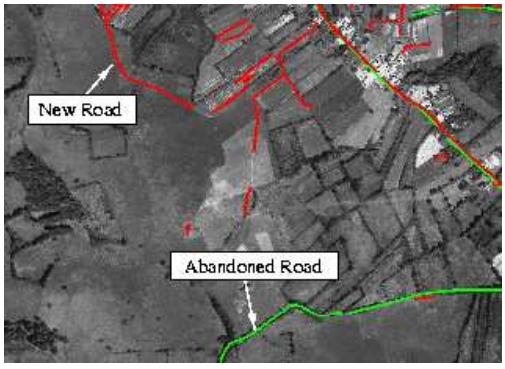

Figure 4: Lines detected on KVR (Green) and Daedalus (Red) projected on the Daedalus image (channel 4).

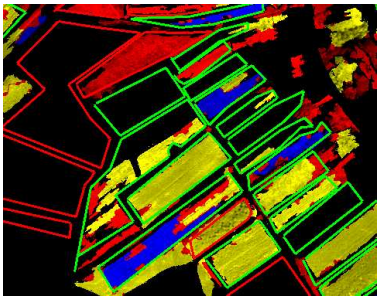

Figure 5: Detection of fields with parallel structure. Blue regions: detected parallel structure, Red regions: No parallel structure, Yellow regions: Doubt, Green lines: Ground truth of used fields, Red lines: Ground truth of unused fields

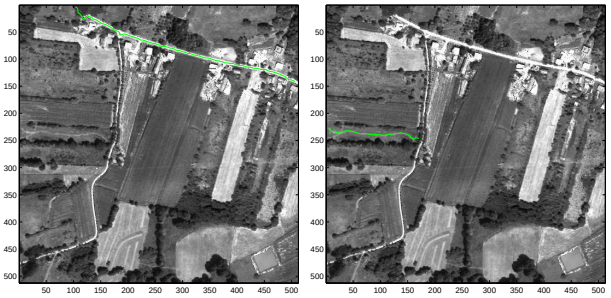

(a) (b)

Figure 6: Two tracking results: (a) on a main road; (b) on a small path .

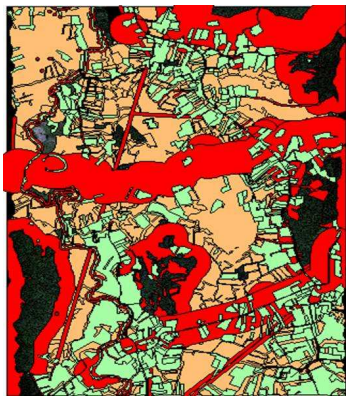

Figure 7: Discrete 'danger map' of Glinska Poljana (preliminary) Red: Danger (Buffers) Orange: Danger (Areas no longer in use) Green: No danger (residential areas, cultivated areas...) Other: No status (forests)